



■ BIOMECHANICS

Experimental and numerical investigation into the influence of loading conditions in biomechanical testing of locking plate fracture fixation devices

**A. MacLeod,
A. H. R. W.
Simpson,
P. Pankaj**

*The University of
Edinburgh, Edinburgh,
United Kingdom*

Objectives

Secondary fracture healing is strongly influenced by the stiffness of the bone-fixator system. Biomechanical tests are extensively used to investigate stiffness and strength of fixation devices. The stiffness values reported in the literature for locked plating, however, vary by three orders of magnitude. The aim of this study was to examine the influence that the method of restraint and load application has on the stiffness produced, the strain distribution within the bone, and the stresses in the implant for locking plate constructs.

Methods

Synthetic composite bones were used to evaluate experimentally the influence of four different methods of loading and restraining specimens, all used in recent previous studies. Two plate types and three screw arrangements were also evaluated for each loading scenario. Computational models were also developed and validated using the experimental tests.

Results

The method of loading was found to affect the gap stiffness strongly (by up to six times) but also the magnitude of the plate stress and the location and magnitude of strains at the bone-screw interface.

Conclusions

This study demonstrates that the method of loading is responsible for much of the difference in reported stiffness values in the literature. It also shows that previous contradictory findings, such as the influence of working length and very large differences in failure loads, can be readily explained by the choice of loading condition.

Cite this article: *Bone Joint Res* 2018;7:111–120.

Keywords: Fracture healing, Strain, Boundary conditions

■ A. MacLeod, PhD, Research Associate, The University of Edinburgh,
■ P. Pankaj, PhD, Professor of Computational Biomechanics, The University of Edinburgh, School of Engineering, Institute for Bioengineering, Faraday Building, Edinburgh EH9 3DW, UK.
■ A. H. R. W. Simpson, BA, BM, BCh, MA, FRCSEd, DM, George Harrison Law Professor of Orthopaedic Surgery, Department of Orthopaedic Surgery, University of Edinburgh, Chancellor's Building, 49 Little France Crescent, Old Dalkeith Road, Edinburgh EH16 4SB, UK.

Correspondence should be sent to P. Pankaj;
email: pankaj@ed.ac.uk

doi: 10.1302/2046-3758.71.BJR-2017-0074.R2

Bone Joint Res 2018;7:111–120.

Article focus

- The influence that the method of restraining and load application has on the stiffness of the bone-plate system *in vitro*.
- The effect of loading conditions on the strain distribution within the bone and the stresses in the implant.

Key messages

- The method of loading is responsible for much of the difference in reported stiffness values in the literature.
- Previous contradictory findings, such as the influence of working length and very large differences in failure loads, can be

readily explained by the choice of loading condition.

Strengths and limitations

- This is an experimental and validated finite element simulation study evaluating a range of widely used *in vitro* testing conditions.
- The study does not address the *in vivo* condition, but speculates as to the most appropriate *in vitro* loading condition.

Introduction

Secondary fracture healing is strongly influenced by the interfragmentary motion (IFM)

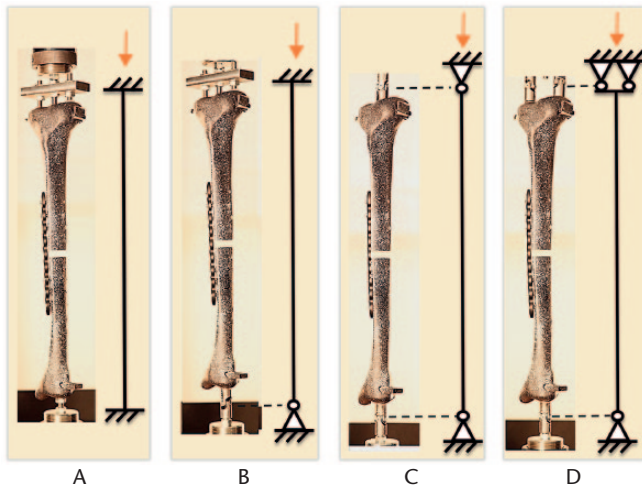


Fig. 1

Photographs of the four loading conditions tested and the corresponding engineering symbols: loading condition A, with clamped ends proximally and distally; loading condition B, with clamped end proximally and pinned end distally; loading condition C, with pinned ends proximally and distally; and loading condition D, with a hinge proximally and a pin distally. The speckled pattern on the surface of the composite tibia was used for digital image correlation.

between fractured bone segments.¹ A controlled amount of axial motion is known to be beneficial for the healing process,^{2,3} whereas shear or torsional motions have been shown to be disruptive.^{3,4} It is important to be able to determine accurately the amount of axial movement a fixator will produce at the fracture site, as too much or too little can cause nonunion.^{3,5}

Interfracture motion depends on the stiffness of the bone-fixator system; however, stiffness defined as the slope of the load-displacement curve has been evaluated by several different methods and reported in the fixation literature. First, most studies use the secant line to evaluate stiffness, which is obtained from the applied load divided by the displacement at a chosen location. Second, the point chosen to determine the displacement can influence its value considerably.⁶ In this study, the term 'axial stiffness' will imply that the displacement is being measured at the loading actuator, whereas stiffness evaluated from maximal fracture gap closure (or IFM) will be called 'gap stiffness'. Stiffness is useful for comparisons between studies because comparing the IFM alone does not take into consideration the level of loading. The range of values of stiffness reported in the literature for locked plating (also known as locking compression plating) vary by three orders of magnitude.⁷⁻¹⁷ Several factors have been shown to influence the IFM produced by a locking plate: the geometry and material of the plate;¹⁸ the bone-plate off-set;⁹ and the position of screws within the plate.⁷ This wide variation, however, cannot be readily explained solely on the basis of studies' differing materials, geometries and methods of stiffness evaluation.

One aspect of mechanical testing that has a strong influence on stiffness evaluation but has received

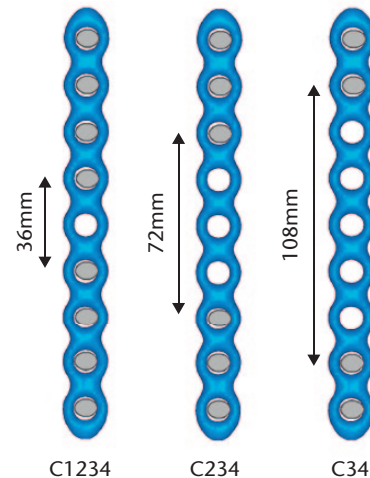


Fig. 2

The three screw arrangements evaluated in the study, showing the size of the working length in each case.

relatively little attention is the way that bone samples are restrained and loaded during tests. Bone samples that are fully restrained (or potted) at the ends will provide displacements that are significantly different from tests in which bone ends are pinned (allowing rotation). The use of fully restrained boundary conditions in computer simulation has been criticized;^{19,20} nevertheless, many biomechanical studies of locking plates use clamped or potted loading conditions to make predictions of fracture gap motion, implant strength, and fatigue resistance.^{9,10,12-14,16,21-25} Predictions of stiffness in studies using a similar loading condition, for example where both ends of the specimen are pinned, are generally confined to differences within a single order of magnitude.^{7,11,15,18,26} The influence of *in vitro* testing conditions must be understood so that results can be interpreted in context.

In addition to the wide range of IFM predictions, previous studies have produced other conflicting results. In a study with titanium femoral locking plates loaded in axial compression, Hoffmeier et al⁸ found failure loads between 385 N and 391 N, whereas in another study by Liang et al,²³ specimens withstood loads of between 4250 N and 4600 N. A previous study by Stoffel et al⁷ has shown working length (the distance between the two innermost screws) to have a dramatic influence on stiffness and fatigue resistance, but other studies report almost no influence.^{8,22} Peak strains within the bone were predicted to be located around screws farthest away from the fracture gap in some studies,^{10,27,28} but others have found them to be located at the screws nearest the fracture site.^{6,7,29}

The aim of this study is to inform on the importance of the loading conditions in experimental or numerical bone tests. Experimental and computational models of the bone-plate system are used to examine the influence that

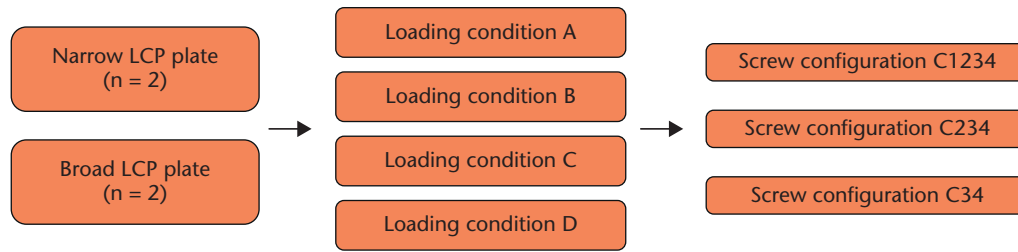
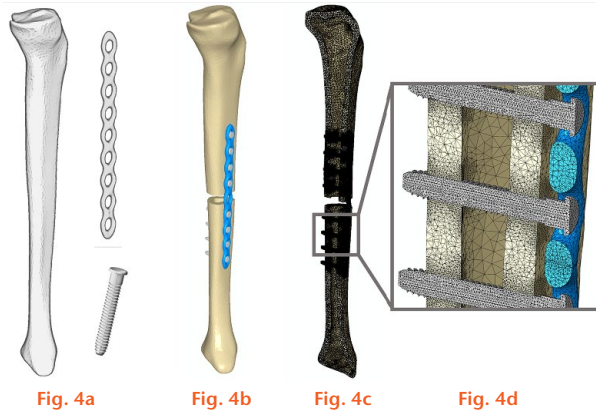


Fig. 3

The testing regime used for the composite tibia specimens. Two locking compression plate (LCP) types, four loading conditions, and three screw configurations were evaluated.



a) 3D geometries of the composite tibia, plate, and screws; b) the finite element model; c) the meshed model; and d) the mesh resolution at the screw-bone interface.

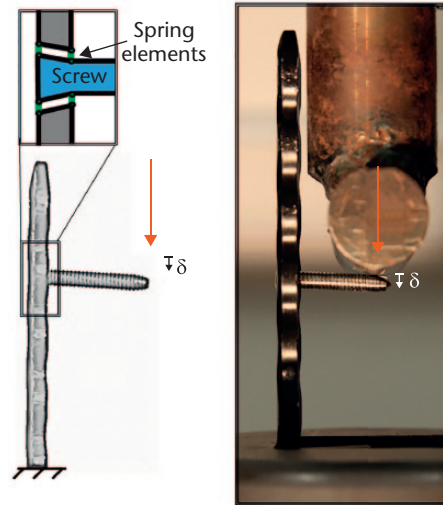


Fig. 5a

Fig. 5b

a) The finite element representation of the screw-plate interface; b) the experimental setup to validate the spring elements used to model the interaction.

the method of restraining and load application has on the IFM produced. This study also uses finite element (FE) analyses to examine the effect of loading conditions on the strain distribution within the bone and the stresses in the implant. While this study speculates which of the several experimental loading scenarios examined is closest to the *in vivo* condition, it does not attempt to recreate it.

Materials and Methods

In vitro studies. Composite tibias (fourth-generation large Sawbones tibia #3402, Sawbones Europe AB, Malmö, Sweden) were implanted with narrow ($n=2$) and broad ($n=2$) steel locking plates and screws (AxSOS Locking Plate System; Stryker, Kalamazoo, Michigan). We experimentally determined the second moments of area in the weak axis to be 50.6 mm^4 and 96.9 mm^4 for the narrow and broad plates, respectively.^{30,31} The plates were fitted by an orthopaedic surgeon (who was not an author on this paper) and offset 2 mm from the bone. A 10 mm osteotomy of the diaphysis was used.^{11,18,32} The specimens were 405 mm long, with an outer bone width at the fracture site of 28 mm. The locking screw dimensions were 5.0 mm external and 4.3 mm core diameter. The pilot hole was the same size as the internal diameter as recommended by the manufacturer. Threads had a depth of 0.7 mm and a spacing of 1.2 mm. Each

implanted specimen was tested using four different loading conditions (Fig. 1).

Condition A: clamped proximally, clamped distally, where both ends of the bone are restrained against rotation. Previous studies that have used this condition for *in vitro* testing include Strauss et al¹⁶ and Yanez et al.²⁵

Condition B: clamped proximally, pinned distally, where the proximal tibia is restrained against rotation and the ankle is free to rotate. Previous studies that have used this condition for *in vitro* testing include Bottlang et al,¹⁰ Chao et al,²² Liang et al,²³ and Granata et al.²¹

Condition C: pinned proximally, pinned distally, where both ends of the bone are free to rotate. Previous studies that have used this condition for *in vitro* testing include Stoffel et al,⁷ Hoffmeier et al,⁸ and Zlowodzki et al.³³

Condition D: hinged proximally, pinned distally; medial and lateral condylar restraint was provided, permitting rotation in the sagittal plane proximally while the ankle is free to rotate. A previous study that used this condition for *in vitro* testing was Assari et al.³⁴

Universal joints were used to allow rotation, and positioned 20 mm from the articular surfaces of the tibias,

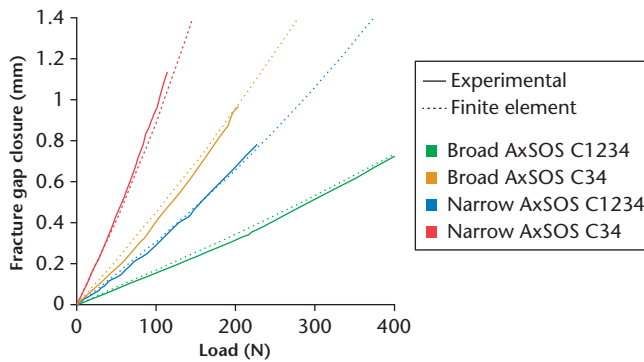


Fig. 6

The load-displacement plots for the experimental and finite element cases using loading condition C. Results are shown for the two plate types (Stryker AxSOS broad and narrow plates), and for the shortest and longest working lengths evaluated in the study.

making the effective length of the specimens 445 mm for conditions C and D. For the clamped conditions, the bone was bolted directly into the test machine, resulting in an effective length of 405 mm. In all cases, the fittings were secured to the bone using M8 steel bolts and a 10 mm thick steel plate within the metaphysis. While many studies have used idealized bone models, such as cylinders,^{7,10,11,13,15,25} the reason for modelling the whole tibia was to situate the boundary conditions at the relevant anatomical locations. It was expected that the bone length and shape would alter the stiffness prediction and this was later confirmed.

For each loading condition, three tests were conducted corresponding to different screw configurations, which are summarized in Figure 2. Screw configuration 'C1234' indicates that screws were placed in holes one to four counting from the fracture site. In all cases, the screw configurations were symmetrical on either side of the fracture. The specimens were loaded at a rate of 5 N/s using an Instron 4505 testing frame (Instron, Norwood, Massachusetts). A black-on-white speckled paint pattern was applied to the surface of the bone. A camera (EOS 5D Mark II 21.1 megapixel digital single-lens reflex (SLR); Canon (UK) Ltd, Surrey, United Kingdom) was positioned at the height of the osteotomy site; the specimen was aligned such that the dominant plate deformation during testing was in the plane of view. Photos were taken at regular load intervals (25 N) during testing. Fracture gap motions were obtained using digital image correlation software GeoPIV in Matlab 7.6 (MathWorks, Cambridge, United Kingdom).³⁵ The accuracy of this method was evaluated using a rigid body motion test; this demonstrated that we could achieve an accuracy of ± 0.02 mm. The axial movement at the fracture gap (IFM) was evaluated at the cortex furthest away from the plate for each loading configuration and screw configuration (transverse motions also provided in Supplementary figure 1). The testing regime for each specimen is summarized in Figure 3. For each specimen ($n=2$ for narrow plates and

broad plates), there were four loading conditions and three screw arrangements tested (12 tests), resulting in a total of 48 tests. The IFM was recorded at 200 N, except for screw configuration C34, which was recorded at 100 N due to the large deformations.

The gap stiffness was evaluated for each loading condition and for each screw configuration using the applied load divided by the IFM. These values were compared with previous studies that predicted the stiffness of locking plates *in vitro*.^{7–16,18,22–26,28,34,36–40}

Finite element simulation. A 3D finite element model was developed based on the experimental models (Fig. 4). The geometry of the tibia and plates were obtained using a desktop 3D laser scanner (NextEngine, Santa Monica, California). This surface was offset by 5 mm internally to produce the cortical shell. As the simulated fracture was in the tibial diaphysis, screw anchorage is provided by cortical bone.³⁶ As such, only the cortical bone was included in the models (Fig. 4).^{29,41} The Sawbones cortex was given a Young's modulus of 16.35 GPa, based on a mean of the tensile and compressive moduli.⁴² The steel was assigned a Young's modulus of 180 GPa. All materials were assumed to be homogeneous, isotropic, and linear elastic, and were assigned a Poisson's ratio of 0.3.^{36,43}

The screw threads were modelled as rings rather than helical,⁶ and screw-bone interaction used a Coulomb friction coefficient of 0.3.^{44,45} It has been previously shown that, in locking plates, although the screw head is locked into the plate's threaded chamber, the two cannot be assumed to be monolithic or completely bonded.^{30,46} To model the plate-screw interaction, the predicted displacement at the tip of the screw was evaluated for the FE model (Fig. 5a) and compared with experiments in which the screw was subjected to a force (Fig. 5b).^{30,31} It was found that the assumption of a fully bonded plate-screw interface resulted in the FE model being approximately eight times stiffer than the experiments. The interface was modelled using eight spring elements (four each, both top and bottom) around the screw head, connecting to the plate (Fig. 5a). A linear spring stiffness of 10 kN/mm per spring produced the closest match to the experimental results.

The models used over 1.3 million linear elements, and 81 000 quadratic tetrahedral elements with refinement around screw holes. In the region around screw holes, the mean element edge length was 0.3 mm to 0.4 mm. A mesh convergence study was performed and the results showed that doubling mesh density of the plate only increased the fracture gap motion by 0.3%. Similarly, when doubling the mesh resolution in the bone, the change in peak minimum (and maximum) compressive strain was 3.0% (2.1%), and the increase in fracture gap motion was 4.5%. The analyses were conducted using geometrical nonlinearity using Abaqus 6.10 (Simulia, Providence, Rhode Island).

Table 1. Experimental gap stiffness (load divided by interfragmentary motion at the far cortex) for the different loading conditions, plate types, and screw configurations evaluated in the study

Plate type and screw configuration	Gap stiffness (N / mm)				Load (N)	Error (%)
	Experimental T1	Experimental T2	Mean	Finite element		
Loading condition A						
Narrow AxSOS						
C1234	1008.7	908.0	958.3	3342.6	200	248.8
C234	950.3	613.5	781.9	3076.4	200	293.4
C34	680.5	440.6	560.5	2785.6	100	396.9
Broad AxSOS						
C1234	1398.9	1297.0	1347.9	3495.5	200	159.3
C234	534.7	1029.7	782.2	3174.5	200	305.8
C34	701.6	989.5	701.6	2834.1	100	303.9
Loading condition B						
Narrow AxSOS						
C1234	764.6	985.6	875.1	3249.5	200	271.3
C234	596.6	613.1	604.8	3014.5	200	398.4
C34	425.1	553.2	489.2	2564.6	100	424.3
Broad AxSOS						
C1234	1063.2	776.1	919.7	3334.1	200	262.5
C234	684.9	769.5	727.2	2927.9	200	302.6
C34	462.3	301.2	462.3	2407.7	100	420.8
Loading condition C						
Narrow AxSOS						
C1234	299.0	366.5	332.8	323.6	200	-2.7
C234	269.7	216.5	243.1	185.1	200	-23.9
C34	114.1	105.0	109.6	112.9	100	3.0
Broad AxSOS						
C1234	628.5	744.7	686.6	580.4	200	-15.5
C234	374.0	323.0	348.5	337.5	200	-3.2
C34	210.1	467.7*	210.1	209.0	100	-0.6
Loading condition D						
Narrow AxSOS						
C1234	556.8	426.2	491.5	931.9	200	89.6
C234	388.3	377.5	382.9	638.9	200	66.9
C34	273.6	257.2	265.4	375.0	100	41.3
Broad AxSOS						
C1234	946.0	742.3	844.1	1132.2	200	34.1
C234	708.4	555.6	632.0	734.9	200	16.3
C34	397.4	403.0	397.4	434.0	100	9.2

*This value was excluded from the mean stiffness and error calculation as bone-plate contact occurred during deformation

The FE models were used to predict the IFM in an identical manner to experimental tests, incorporating the different plate geometries, boundary conditions, and screw configurations. Additionally, to examine the influence of loading conditions on the internal stress-strain environment, the load was increased to 500N. This increased load was selected to represent partial weight-bearing in the early stages of healing where the fixator is transmitting most of the load.⁴⁷

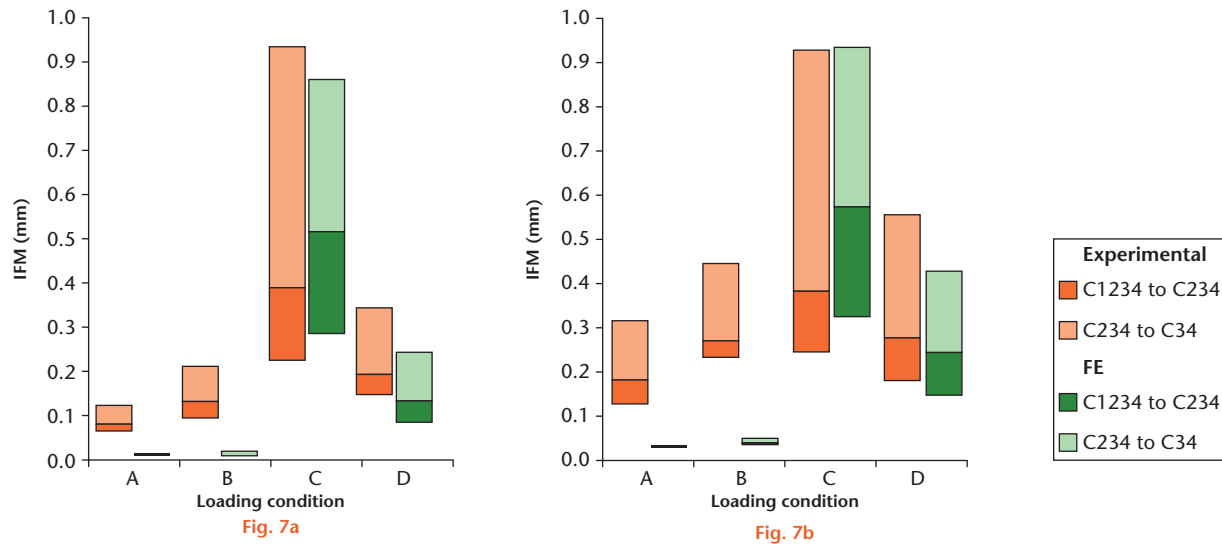
Results

To validate the FE models, the load-deformation response of loading condition C (Fig. 1c) was used; the comparison is shown in Figure 6. There was good agreement with the experimentally predicted stiffness results, with the maximum difference of 23.9% for all screw configurations and plate types (Table I).

The axial IFM predictions for each loading condition are shown in Figure 7. In each case, the influence of screw placement is shown by the size of the bar (the lower

value is the motion with C1234; the higher is with C34). Taking a mean of all screw configurations and plate types, the finite element IFM predictions of conditions C (rotation allowed at both ends) and D (rotation allowed distally and hinged proximally) were within 9% and 22% of the experimental results, respectively. On the other hand, the FE predictions for conditions A (fully clamped) and B (clamped proximally and pinned distally) were approximately two to three times smaller than those of the experimental tests. Our experimental tests showed that the choice of loading condition alone could alter the gap stiffness prediction by nearly three times for the smallest working length, and six times for the largest working length. In FE simulations, the observed differences were much larger (as much as 24 times), as the clamp in FE models is ideally rigid. This is very difficult to achieve in *in vitro* experiments. Translational IFM predictions are provided in Supplementary figure 1.

The experimental gap stiffness predictions are shown against values from the literature in Figure 8. The last four



The mean experimentally measured axial interfragmentary motion (IFM) and predictions using the finite element (FE) simulation for each loading condition and screw configuration considered in the study for a) the narrow locking plate using a load of 100N, and b) the broad locking plate using a load of 200N.

bars corresponding to the present study have the upper value of stiffness evaluated from screw configuration C1234 and the lower value derived from C34.

Minimum principal strain was examined for the various loading scenarios on the surface of the bone underneath the plate (Fig. 9). Minimum principal strain was chosen because compressive strains dominate within the bone under axial loading. Each loading condition produces a unique pattern of strain within the bone around the screw hole locations. The peak compressive strains were 0.36%, 0.31%, 0.28%, and 0.51% for loading conditions A, B, C, and D, respectively. For loading conditions A and B, the peak strains were located around the screw farthest from the fracture, whereas for loading conditions C and D, the peak strains were located around the screw closest to the fracture.

The von Mises stress was plotted for the screws and plate for each loading condition using screw configuration SC1234 at a load of 500N (Fig. 10). The maximum stress within the narrow plate was 53 MPa, 58 MPa, 603 MPa, and 295 MPa for loading conditions A, B, C, and D, respectively. Loading condition C produced large regions of high stress as the plate is free to bend. Loading conditions A and B resulted in much smaller plate stresses as they are prevented from bending, thus carrying predominantly axial stress. Loading condition D resulted in biaxial bending and had smaller regions of high stress than condition C.

Discussion

Experimental and numerical models of fractured bone implanted with fixation devices were used to make predictions of IFM and stiffness, strength of implants, and

strain within the bone. This study shows that the method of load application can have substantial influence on IFM and stiffness predictions in locking plate constructs. This study also demonstrates for the first time that the pattern of strains within the bone, as well as the stresses within the metalwork, is strongly influenced by the choice of loading condition.

All of the restraint conditions examined in the present study have been previously employed in the experimental testing literature.^{7,8,10,11,21-23,25,33} It is evident that studies using clamped approaches (conditions A and B) produced the highest stiffness and lowest plate stresses as they restrict plate bending.^{10,13,24,48} Studies using the pinned approach (condition C), on the other hand, allowed the plate to bend freely, producing the lowest stiffness and highest stresses.^{7,8,15,18} While the previous studies considered in Figure 8 are not directly comparable, the range of stiffness values quoted varies by three orders of magnitude; predictions of stiffness for studies using loading condition C are generally confined to within a single order of magnitude.^{7,11,15,18,26} Condition C also produced a nonlinear deformation response with increasing load. This was captured by the geometrically nonlinear FE analysis conducted. The IFM produced using condition B (Fig. 7b) was very similar to that of condition A (Fig. 7a). This shows that the clamped boundary condition dominated the behaviour. Bottlang et al¹⁰ used a mean value of IFM (taking a mean of the motion at the near and far cortices) for their stiffness prediction; using the maximum value reduces their axial stiffness prediction by approximately 40%, but it still remains much larger than the majority of the studies (Fig. 8). In the present study, condition D produced stiffness values in

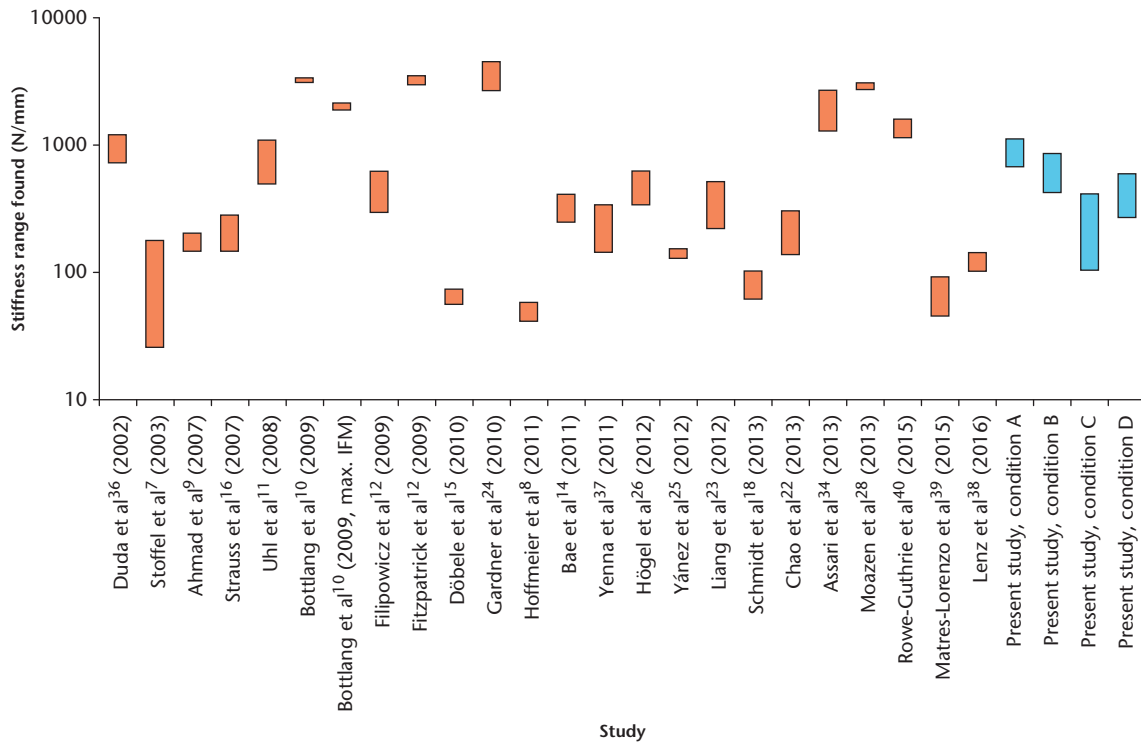


Fig. 8

The recorded stiffness values of locking plate constructs found by previous studies (orange bars) and the stiffness values of each of the loading conditions used in this study (blue bars). IFM, interfracture motion.

between the extremes represented by the other loading conditions (Fig. 8). However, this condition was used by Assari et al,³⁴ and their stiffness values are at the upper end of the range found in the literature. Differences between the loading conditions become even more pronounced when considering the influence of different screw arrangements (Fig. 7). Condition C was sensitive to changes in working length (distance between innermost screws), while conditions A and B were relatively insensitive. This explains the comparatively small differences between working lengths observed by Chao et al²² (using condition A) and the much larger difference predicted by Stoffel et al⁷ (using condition C).

In a study of various unilateral fixators, Epari et al⁴⁹ found that fixators which had ‘moderate’ axial stiffness (2000 N/mm) and ‘high’ shear stiffness (500 N/mm) produced the best healing outcomes in terms of residual torsional stiffness. These values are at the upper end of the stiffness range presented in the literature and must be taken in the context of the loading condition used to evaluate them. In their study, both ends of the bones were potted in poly(methyl methacrylate) (PMMA), representing a clamped condition. The use of a clamped condition implies unrealistic rotational rigidity at the knee and ankle, and it restricts plate bending and therefore cannot be used for predictions of IFM.

Some studies have used a clamped condition comparing newer ‘flexible’ locking screw types with standard

locking screws.^{10,13,15,24} In these studies, the plate bending will be restricted, thus exaggerating the differences in IFM found between the types of screw tested. Differences in loading conditions may also explain the large differences in failure loads found by various studies. Pinned studies such as Hoffmeier et al⁸ and Zlowodzki et al³³ predict static failure loads between 385 N and 1126 N. In clamped studies, Liang et al²³ found mean static failure loads of 4438 N.

As many of the previous studies considered had different lengths of test specimen, the influence that bone length had on the motion prediction was investigated. The FE model using loading condition C was re-run positioning the end conditions closer to the fracture gap and constraining them to the shaft. A 42.6% reduction in bone length resulted in a 31% reduction in gap motion. In addition, it is likely that the fracture location would change the fracture gap motion prediction, i.e. if the fracture was closer to the end of the bone. The Young’s modulus of the bone is also known to influence the axial stiffness of bone-plate systems; however, its influence on IFM is much smaller,¹¹ particularly for values close to human cortical bone.³⁰

This study did not attempt to recreate the *in vivo* loading scenario, but evaluated the influence of different *in vitro* loading conditions. Ideally, the inclusion of all muscles, appropriate joint reactions, and the presence of fracture callus would reveal the true nature of the *in vivo*

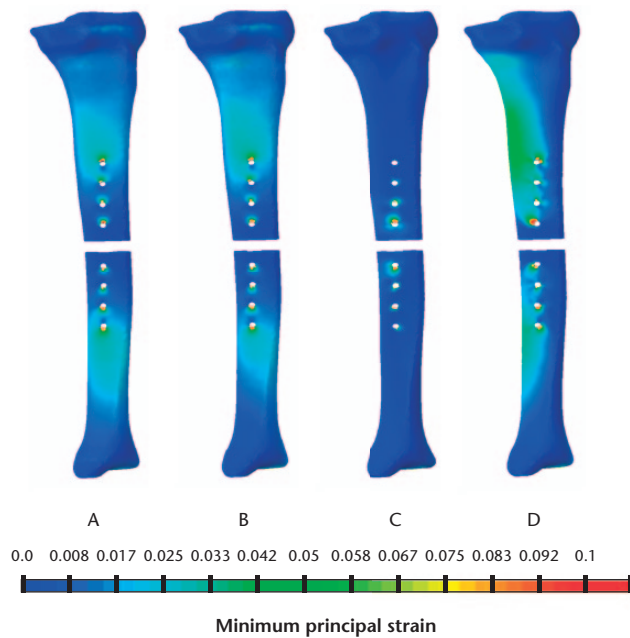


Fig. 9

The predicted minimum principal strains within the bone using screw configuration C1234 at a load of 500N. The letters A to D correspond with the loading conditions considered in this study.

mechanical response. However, this is not straightforward, and simplified loading conditions will continue to be used in experiments and provide biomechanical guidance on fracture fixation. In condition D, restraint was provided at both condyles to produce the hinge; this was to mimic the condylar joint reactions at the knee as opposed to a single knee joint reaction. As the thin dimension of the plate was in a different plane to the rotation allowed at the knee, condition D resulted in biaxial bending of the plate. The authors believe that the true physiological joint restraint is likely to be in between conditions C and D.

As shown, the peak strains within the bone around screw holes are the highest at the screw closest to the fracture gap for condition C (Fig. 9c). This is consistent with a recent study by Donaldson et al²⁹ on unilateral fixators that predicted the highest degree of yielding and associated loosening at this location. Conversely, studies using clamped conditions^{10,27,28} predicted the highest strains at the screw farthest from the fracture (Figs 9a and 9b). While periprosthetic fractures are known to occur at this location, they have been attributed to osteoporotic bone and/or excessive plate rigidity.⁵⁰ Additional simulations confirmed that both reducing the Young's modulus of bone and increasing plate rigidity increased the level of strain within the bone at the plate ends, even when using loading condition C. Condition D produced large strains both near and far from the fracture site.

This study has a few limitations. It only considers axial loading, and boundary conditions may influence the response in a different way for bending and torsional

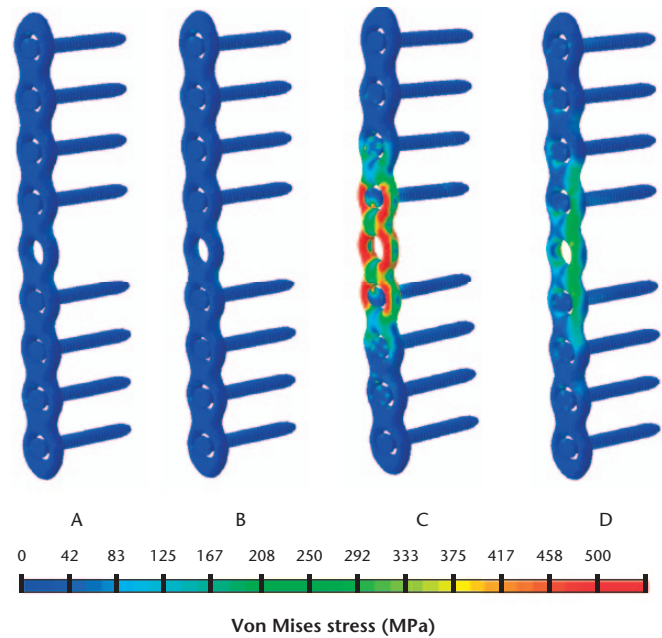


Fig. 10

The predicted von Mises stress within the plate using screw configuration C1234 at a load of 500N. The letters A to D correspond with the loading conditions considered in this study.

loading conditions; these can arise due to a range of different physiological activities. We recommend that future studies should also investigate the influence of bending and torsional loading regimes. While the study highlights the influence of boundary conditions on the bone-plate system, it does not recreate the *in vivo* environment, which can be a complex mix of some of these idealized conditions. Some previous studies have validated computational models of intact cadaveric bones under different loading regimes.^{51,52} The present study considered fixation constructs, which are influenced by changes in loading and restraint due to the lower construct stiffness. Additionally, load-displacement effects become non-linear due to the eccentrically located plate.⁵³ Therefore, it would be valuable to confirm the findings of this study using a cadaveric model, although it is unlikely that the use of cadaveric bone would change our conclusions relating to construct stiffness or plate stress.³¹ On the other hand, the variation in material properties would alter the strains in the bone around the screws. The study is limited to the period in which no healing has taken place. The role of boundary conditions is very likely to change once callus formation has been initiated. We did not include material nonlinearity in the FE models as the loading considered did not cause the metalwork to reach the yield stress, or cause the bone to reach the yield strain. In addition, we considered only short-term static loading; for long-term predictions, viscoelasticity or fatigue effects may play a role.

Many previous studies have used clamped loading conditions.^{9,10,12-14,16,21-25} This study showed that clamped

loading conditions were relatively insensitive to the positioning of screws. In our experimental tests, some motion was seen from the digital image correlation, which revealed that the clamp was not completely restraining movement. Consequently, the experimental stiffness for loading conditions A and B was much smaller than that of the FE modelling, which assumes perfect clamps. Studies that choose to use such loading conditions must be aware that the rigidity of the clamp or potting material may be more influential than any of the other variables being examined. Additionally, computational studies must be aware that modelling representations of clamped boundary conditions will generally be much more rigid than reality and therefore make validation challenging. The hinged condition fully restrains the bone in the direction perpendicular to the hinge and therefore may not be readily replicated in experiments. Thus, the authors believe that the most readily comparable results from different studies are from condition C, where the bone ends can rotate freely. Since both the knee and the ankle joints allow some rotation in all directions, condition C is also close to the *in vivo* scenario. To improve comparisons further, studies that use condition C should quote the distance between the centres of rotation at the joints and the position of the fracture relative to the joints in addition to other measurements regarding the test set-up. Condition C can also be used to create moments at the joints by using eccentric loading.^{18,26,54} To avoid the large variation in predictions between studies and conflicting results, we recommend that loading condition C, where both ends of the bone are free to rotate, is used as the standard for the *in vitro* evaluation of fractured bone specimens under axial loading.

Supplementary material

 The transverse IFM results are available alongside this article at www.bjr.boneandjoint.org.uk

References

1. Wagner M. General principles for the clinical use of the LCP. *Injury* 2003;34(Suppl 2):B31-B42.
2. Kenwright J, Richardson JB, Goodship AE, et al. Effect of controlled axial micromovement on healing of tibial fractures. *Lancet* 1986;2:1185-1187.
3. Gaston MS, Simpson AH. Inhibition of fracture healing. *J Bone Joint Surg [Br]* 2007;89-B:1553-1560.
4. Augat P, Burger J, Schorlemmer S, et al. Shear movement at the fracture site delays healing in a diaphyseal fracture model. *J Orthop Res* 2003;21:1011-1017.
5. Kenwright J, Gardner T. Mechanical influences on tibial fracture healing. *Clin Orthop Relat Res* 1998;355S(Suppl):S179-S190.
6. MacLeod AR, Pankaj P, Simpson AH. Does screw-bone interface modelling matter in finite element analyses? *J Biomech* 2012;45:1712-1716.
7. Stoffel K, Dieter U, Stachowiak G, Gächter A, Kuster MS. Biomechanical testing of the LCP—how can stability in locked internal fixators be controlled? *Injury* 2003;34(Suppl 2):B11-B19.
8. Hoffmeier KL, Hofmann GO, Mückley T. Choosing a proper working length can improve the lifespan of locked plates. A biomechanical study. *Clin Biomech (Bristol, Avon)* 2011;26:405-409.
9. Ahmad M, Nanda R, Bajwa AS, et al. Biomechanical testing of the locking compression plate: when does the distance between bone and implant significantly reduce construct stability? *Injury* 2007;38:358-364.
10. Bottlang M, Doornink J, Fitzpatrick DC, Madey SM. Far cortical locking can reduce stiffness of locked plating constructs while retaining construct strength. *J Bone Joint Surg [Am]* 2009;91-A:1985-1994.
11. Uhl JM, Seguin B, Kapatkin AS, et al. Mechanical comparison of 3.5 mm broad dynamic compression plate, broad limited-contact dynamic compression plate, and narrow locking compression plate systems using interfragmentary gap models. *Vet Surg* 2008;37:663-673.
12. Filipowicz D, Lanz O, McLaughlin R, Elder S, Werre S. A biomechanical comparison of 3.5 locking compression plate fixation to 3.5 limited contact dynamic compression plate fixation in a canine cadaveric distal humeral metaphyseal gap model. *Vet Comp Orthop Traumatol* 2009;22:270-277.
13. Fitzpatrick DC, Doornink J, Madey SM, Bottlang M. Relative stability of conventional and locked plating fixation in a model of the osteoporotic femoral diaphysis. *Clin Biomech (Bristol, Avon)* 2009;24:203-209.
14. Bae JH, Oh JK, Chon CS, et al. The biomechanical performance of locking plate fixation with intramedullary fibular strut graft augmentation in the treatment of unstable fractures of the proximal humerus. *J Bone Joint Surg [Br]* 2011;93-B:937-941.
15. Döbele S, Horn C, Eichhorn S, et al. The dynamic locking screw (DLS) can increase interfragmentary motion on the near cortex of locked plating constructs by reducing the axial stiffness. *Langenbecks Arch Surg* 2010;395:421-428.
16. Strauss EJ, Alfonso D, Kummer FJ, Egol KA, Tejwani NC. The effect of concurrent fibular fracture on the fixation of distal tibia fractures: a laboratory comparison of intramedullary nails with locked plates. *J Orthop Trauma* 2007;21:172-177.
17. Wähnert D, Windolf M, Brianza S, et al. A comparison of parallel and diverging screw angles in the stability of locked plate constructs. *J Bone Joint Surg [Br]* 2011;93-B:1259-1264.
18. Schmidt U, Penzkofer R, Bachmaier S, Augat P. Implant material and design alter construct stiffness in distal femur locking plate fixation: a pilot study. *Clin Orthop Relat Res* 2013;471:2808-2814.
19. Phillips ATM. The femur as a musculo-skeletal construct: a free boundary condition modelling approach. *Med Eng Phys* 2009;31:673-680.
20. Speirs AD, Heller MO, Duda GN, Taylor WR. Physiologically based boundary conditions in finite element modelling. *J Biomech* 2007;40:2318-2323.
21. Granata JD, Litsky AS, Lustenberger DP, Probe RA, Ellis TJ. Immediate weight bearing of comminuted supracondylar femur fractures using locked plate fixation. *Orthopedics* 2012;35:e1210-e1213.
22. Chao P, Conrad BP, Lewis DD, Horodyski M, Pozzi A. Effect of plate working length on plate stiffness and cyclic fatigue life in a cadaveric femoral fracture gap model stabilized with a 12-hole 2.4 mm locking compression plate. *BMC Vet Res* 2013;9:125.
23. Liang B, Ding Z, Shen J, et al. A distal femoral supra-condylar plate: biomechanical comparison with condylar plate and first clinical application for treatment of supracondylar fracture. *Int Orthop* 2012;36:1673-1679.
24. Gardner MJ, Nork SE, Huber P, Krieg JC. Less rigid stable fracture fixation in osteoporotic bone using locked plates with near cortical slots. *Injury* 2010;41:652-656.
25. Yáñez A, Cuadrado A, Carta JA, Garcés G. Screw locking elements: a means to modify the flexibility of osteoporotic fracture fixation with DCPs without compromising system strength or stability. *Med Eng Phys* 2012;34:717-724.
26. Högel F, Hoffmann S, Weninger P, Bühren V, Augat P. Biomechanical comparison of two locking plate systems for the distal tibia. *Eur J Trauma Emerg Surg* 2012;38:53-58.
27. Salas C, Mercer D, DeCoster TA, Reda Taha MM. Experimental and probabilistic analysis of distal femoral periprosthetic fracture: a comparison of locking plate and intramedullary nail fixation. Part A: experimental investigation. *Comput Methods Biomech Biomed Engin* 2011;14:157-164.
28. Moazen M, Mak JH, Jones AC, et al. Evaluation of a new approach for modelling the screw-bone interface in a locking plate fixation: a corroboration study. *Proc Inst Mech Eng H* 2013;227:746-756.
29. Donaldson FE, Pankaj P, Simpson AH. Bone properties affect loosening of half-pin external fixators at the pin-bone interface. *Injury* 2012;43:1764-1770.
30. MacLeod AR. *Modelling and optimising the mechanical conditions for fracture healing using locked plating* (PhD thesis). University of Edinburgh, 2014.
31. MacLeod AR, Simpson AH, Pankaj P. Age-related optimization of screw placement for reduced loosening risk in locked plating. *J Orthop Res* 2016;34:1856-1864.
32. Krishna KR, Sridhar I, Ghista DN. Analysis of the helical plate for bone fracture fixation. *Injury* 2008;39:1421-1436.
33. Zlowszki M, Williamson S, Cole PA, Zardiackas LD, Kregor PJ. Biomechanical evaluation of the less invasive stabilization system, angled blade plate, and retrograde intramedullary nail for the internal fixation of distal femur fractures. *J Orthop Trauma* 2004;18:494-502.

34. **Assari S, Kaufmann A, Darvish K, et al.** Biomechanical comparison of locked plating and spiral blade retrograde nailing of supracondylar femur fractures. *Injury* 2013;44:1340-1345.
35. **White DJ, Take WA, Bolton MD.** Soil deformation measurement using particle image velocimetry (PIV) and photogrammetry. *Geotechnique* 2003;53:619-631.
36. **Duda GN, Mandruzzato F, Heller M, et al.** Mechanical conditions in the internal stabilization of proximal tibial defects. *Clin Biomech (Bristol, Avon)* 2002;17:64-72.
37. **Yenna ZC, Bhadra AK, Ojike NI, et al.** Anterolateral and medial locking plate stiffness in distal tibial fracture model. *Foot Ankle Int* 2011;32:630-637.
38. **Lenz M, Windolf M, Mückley T, et al.** The locking attachment plate for proximal fixation of periprosthetic femur fractures—a biomechanical comparison of two techniques. *Int Orthop* 2012;36:1915-1921.
39. **Matres-Lorenzo L, Diop A, Maurel N, et al.** Biomechanical comparison of locking compression plate and limited contact dynamic compression plate combined with an intramedullary rod in a canine femoral fracture-gap model. *Vet Surg* 2016;45:319-326.
40. **Rowe-Guthrie KM, Markel MD, Bleedorn JA.** Mechanical evaluation of locking, nonlocking, and hybrid plating constructs using a locking compression plate in a canine synthetic bone model. *Vet Surg* 2015;44:838-842.
41. **Donaldson FE, Pankaj P, Simpson AH.** Investigation of factors affecting loosening of Ilizarov ring-wire external fixator systems at the bone-wire interface. *J Orthop Res* 2012;30:726-732.
42. **No authors listed.** Sawbones. Sawbones Biomechanical Test Materials. <https://www.sawbones.com/products/biomechanical/biomechanical-test-materials.html> (date last accessed 11 December 2017).
43. **Ganesh VK, Ramakrishna K, Ghista DN.** Biomechanics of bone-fracture fixation by stiffness-graded plates in comparison with stainless-steel plates. *Biomed Eng Online* 2005;4:46.
44. **Eser A, Tonuk E, Akca K, Cehreli MC.** Predicting time-dependent remodeling of bone around immediately loaded dental implants with different designs. *Med Eng Phys* 2010;32:22-31.
45. **Pessoa RS, Muraru L, Júnior EM, et al.** Influence of implant connection type on the biomechanical environment of immediately placed implants - CT-based nonlinear, three-dimensional finite element analysis. *Clin Implant Dent Relat Res* 2010;12:219-234.
46. **Synek A, Baumbach S, Pahr D.** CT-Based finite element modelling of plated distal radius fracture osteosynthesis: evaluation against experimental measurements. *21st Congress of the European Society of Biomechanics*. 2015.
47. **Vijayakumar V, Marks L, Bremmer-Smith A, Hardy J, Gardner T.** Load transmission through a healing tibial fracture. *Clin Biomech (Bristol, Avon)* 2006;21:49-53.
48. **Kim SH, Chang SH, Jung HJ.** The finite element analysis of a fractured tibia applied by composite bone plates considering contact conditions and time-varying properties of curing tissues. *Compos Struct* 2010;92:2109-2118.
49. **Epari DR, Kassi JP, Schell H, Duda GN.** Timely fracture-healing requires optimization of axial fixation stability. *J Bone Joint Surg [Am]* 2007;89-A:1575-1585.
50. **Leahy M.** When locking plates fail. *AAOS Now* 2010;5:9.
51. **Gray HA, Taddei F, Zavatsky AB, Cristofolini L, Gill HS.** Experimental validation of a finite element model of a human cadaveric tibia. *J Biomech Eng* 2008;130:031016.
52. **Zani L, Erani P, Grassi L, Taddei F, Cristofolini L.** Strain distribution in the proximal Human femur during in vitro simulated sideways fall. *J Biomech* 2015;48:2130-2143.
53. **MacLeod A, Pankaj P.** Computer simulation of fracture fixation using extramedullary devices: an appraisal. In: Doyle B, Miller K, Wittek A, Nielsen PMF, eds. *Computational Biomechanics for Medicine: Fundamental Science and Patient-specific Applications*. Eighth ed. Switzerland: Springer, 2014:87-99.
54. **Gaebler C, Speitling A, Milne EL, et al.** A new modular testing system for biomechanical evaluation of tibial intramedullary fixation devices. *Injury* 2001;32:708-712.

Acknowledgements

- Thanks to N. D. Clement for fitting the implants to the composite bones.

Funding Statement

- This work was supported by Orthopaedic Research UK under Grant ORUK: 469. We gratefully acknowledge the support of the Osteosynthesis and Trauma Care Foundation. We would like to thank Stryker UK for providing the plates. We gratefully acknowledge the support of EPSRC [Grant EP/K036939/1], which provided the computational resources required for this study.

Author Contributions

- A. MacLeod: Designing the study, Performing experimental testing and computer simulations, Drafting and critically reviewing the manuscript.
- A. H. R. W. Simpson: Designing the study, Critically reviewing the manuscript.
- P. Pankaj: Designing the study, Critically reviewing the manuscript.

Conflicts of Interest Statement

- None declared

© 2018 MacLeod et al. This is an open-access article distributed under the terms of the Creative Commons Attribution licence (CC-BY-NC), which permits unrestricted use, distribution, and reproduction in any medium, but not for commercial gain, provided the original author and source are credited.